IEEE Robotics and Automation Letters (RA-L) paper, presented at ICRA 2026, Vienna, Austria. Cite as RA-L paper.

Efficient Training Data Collection for Distance Sensor Arrays Through Data Correction and Augmentation Approaches

Sogo Amagai, Shin'ichi Warisawa, *Member, IEEE*, and Rui Fukui, *Member, IEEE*

***Abstract*—Several machine learning (ML)-based measurement systems have been proposed to estimate difficult-to-measure quantities from the values of distance sensor arrays. However, variations in sensor output characteristics (OCs) can lead to degradation in the estimation accuracy when transferring training data acquired from the original acquisition sensors to new target sensors. Moreover, acquiring training data from target sensors is time and labor intensive. We propose two methods to convert previously collected training data to reflect different OCs, enabling their repeated use. For evaluation, we use a device that estimates the relative position and orientation of vehicles based on the values of distance sensor arrays. The correction approach for the training data based on the OC data reduces the root-mean-square error (RMSE) by up to 23% compared with transferring training data. The augmentation approach transforms the training data into data that include different OCs using a mapping function constructed from a small batch of training data. Furthermore, a method for collecting a small batch of training data to achieve a higher OC conversion accuracy is demonstrated. The RMSE is reduced by up to 58% by the proposed method compared with transferring training data. The results of this study demonstrate the feasibility of the practical applications of ML-based measurement systems using distance sensor arrays, which may facilitate the development of simple and fast calibration methods.**

***Index Terms*—Distance sensor, robot learning, transfer learning.**

I. Introduction

VARIOUS machine learning (**ML**)-based and data-driven measurement systems have been proposed to estimate difficult-to-measure quantities based on the values of distance sensor arrays. These methods find applications in various fields such as proximity perception in robotics [1], [2], [3], [4], biometrics [5], [6], [7], and user interfaces [8], [9], [10]. Fig. 1 outlines the estimation process using ML in a measurement system featuring a distance sensor array. The distance sensor array acquires training data and associates the array values with the quantity to be measured. The output characteristics (**OCs**) of a distance sensor array are included into the training data to be acquired. ML then estimates the desired quantity based on the distance sensor array values. A notable decline in measurement system accuracy occurs with the utilization of alternative training data for ML estimation, herein referred to as direct transfer (**DT**). This decrease in accuracy is due to differences in OCs of the sensors used in training data collection and ML estimation. For example, in infrared distance sensors, the output of each sensor varies depending on the distance and tilt of the object being measured owing to variations in the characteristics of photoelectric conversion elements, such as a complementary metal–oxide–semiconductor image sensor. The OCs of an optical distance sensor depend on distance d to the measured object and tilt φ of the object, as shown in Fig. 2. Amagai et al. obtained a small decrease in ML estimation accuracy when reusing training data from the same sensor set compared with the accuracy after DT [11]. This suggests that the influence of temperature, ambient light, and time shifts on the sensor output is small compared with that of distance and tilt. To reduce the quantities that determine the OCs by surface

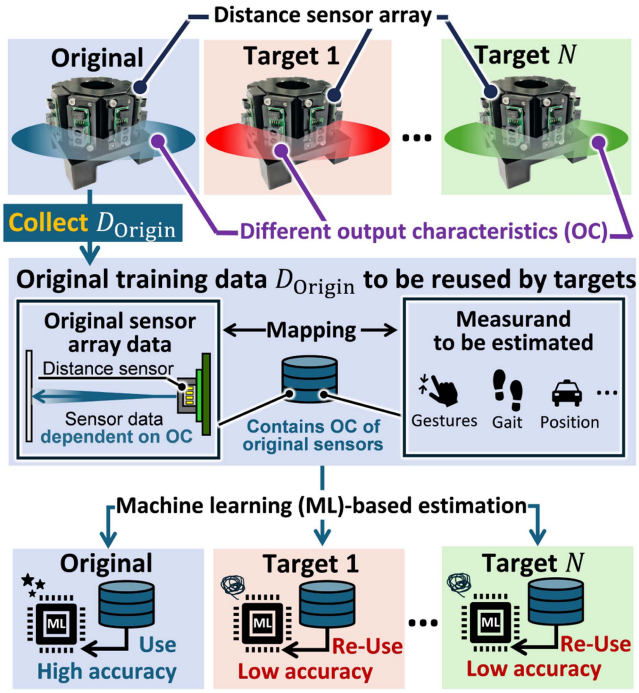

Fig. 1. Schematic of challenge in reusing training data acquired by sensor arrays.

Received 18 September 2024; accepted 28 March 2025. Date of publication 16 April 2025; date of current version 19 May 2025. This article was recommended for publication by Associate Editor E. Johns and Editor A. Faust upon evaluation of the reviewers' comments. *(Corresponding author: Sogo Amagai.)*

The authors are with the Department of Human and Engineered Environmental Studies, Graduate School of Frontier Sciences, The University of Tokyo, Kashiwa 277-8563, Japan (e-mail: amagaisogo@lelab.t.u-tokyo.ac.jp).

Digital Object Identifier 10.1109/LRA.2025.3561567

IEEE Robotics and Automation Letters (RA-L) paper, presented at ICRA 2026, Vienna, Austria. Cite as RA-L paper.

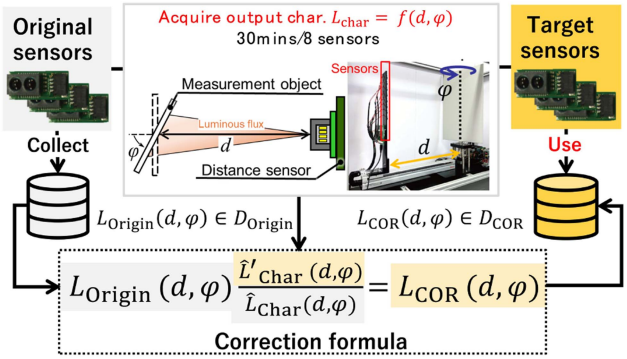

Fig. 2. Training data correction approach (COR).

roughness and reflectance of measured objects, we uniformize the measurement conditions by covering all the surfaces of measured objects with white paper. To prevent a decrease in accuracy, collecting training data for each measurement system is conceivable, but this process is time and labor intensive.

To address the above mentioned problem, two basic approaches are proposed to transform the previously collected training data into data that include different OCs, and their performance is evaluated. The first approach involves correcting the training data once acquired. The training data are corrected based on the OCs of the sensor. The data are acquired by changing the distance and tilt of the object using actuators. The second approach is based on few-shot learning [12], which augments the training data using prior knowledge. This method uses a small amount of training data, which can be collected in a short period, as prior knowledge to construct a mapping function. The mapping function converts the previously collected training data into data that includes OCs of sensors that are used to collect a small batch of training data. This study clarifies the advantages and disadvantages of the two proposed training data conversion approaches.

The contributions of this study are summarized as follows:

- The proposed OC-based training data correction demonstrates less dependence on OC variations between training data compared with other methods.
- The proposed training data augmentation with a mapping function built from a small training set reduces the error by half compared with DT.
- Various guidelines are introduced for acquiring a small batch of training data required to construct a mapping function with high OC conversion accuracy.

The efficacy of the proposed methods is demonstrated using a specific sensor for relative position and orientation measurements. The results of this study are expected to contribute to the practical application of ML-based measurement systems using distance sensor arrays and to the realization of simple and fast calibration methods. The remainder of this letter is organized as follows. Section II discusses related work on improving the efficiency of training data acquisition using sensor data. Section III introduces the training data conversion approaches. Section IV details the ML-based measurement system using a distance sensor array for evaluation. In addition, the experiment described in Section IV demonstrates the impact of experimental condition DT on reducing the estimation accuracy of ML. Sections V and VI describe the implementation of the proposed methods and evaluation experiments, respectively. Finally, Section VII concludes the paper.

II. Related Work

Transfer learning is a popular approach in which a model trained on one task can be applied to a different task. It offers an effective strategy for reducing the effort and time required for training data acquisition [13]. In particular, few-shot learning, which generalizes a model based on limited training data for unseen tasks, is highly effective for streamlining training data acquisition. Few-shot learning applied to training data is realized through data augmentation with prior knowledge [12]. Although some studies have been conducted on sensor data augmentation [14], [15], [16], no method has been identified to address differences in OCs. In domain adaptation for transfer learning, differing OCs in training data establish domain differences. However, to the best of our knowledge, despite the development of domain adaptation for time-series sensor data [17], [18], no method has addressed variations in OCs. Reusing training data requires the time- and resource-demanding process of retraining or fine-tuning a deep neural network (NN) to mitigate discrepancies in OCs. Consequently, practical research on the efficient elimination of training data reacquisition by addressing OC differences is required.

III. Proposed Training Data Conversion Approaches

This section describes the two approaches for converting collected training data into data that reflect different OCs.

A. Training Data Correction Approach

The training data correction approach (COR) corrects distance data based on OC differences. As shown in Fig. 2, data from each sensor in training set D_{Origin} are corrected based on the OC data of the target and original acquisition sensors. The OC data are acquired using an OC acquisition device [11], as shown in the center top of Fig. 2. Data correction is a linear correction of sensor data, as shown in correction formula (1).

$$L_{\text{COR}}(d, \varphi) = L_{\text{Origin}}(d, \varphi) \frac{\hat{L}'_{\text{Char}}(d, \varphi)}{\hat{L}_{\text{Char}}(d, \varphi)} \tag{1}$$

When pair d, φ at the time of distance data acquisition is known, it can be corrected based on the ratio of OC data of the target sensors, L'_{Char}, and those of the original acquisition sensors, L_{Char}. In practice, interpolated OC data $\hat{L}_{\text{Char}}(d, \varphi)$ and $\hat{L}'_{\text{Char}}(d, \varphi)$ are used because the OC data for arbitrary d, φ are required. The estimation accuracy can maintained using D_{COR} in a measurement system composed of target sensors. In COR, the training data need **not** be acquired using the measurement system because only data from the OC acquisition device are required for correction.

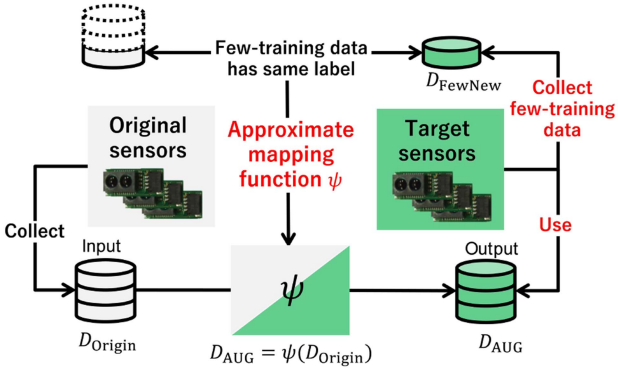

Fig. 3. Few-training data augmentation approach (AUG).

B. Few-Training Data Augmentation

Few-training data augmentation (AUG) converts collected training data into data that reflect different OCs using mapping function ψ that was constructed based on a small batch of training data acquired by target sensors in a short time. As shown in Fig. 3, multi-input and multi-output mapping function ψ is constructed from training data $D_{\text{FewOrigin}}$ created using the original sensors and a small batch of training data D_{FewNew} including the OCs of the target sensors acquired in a short time. Using the constructed multi-input and multi-output mapping function, ψ, D_{FewNew} is augmented to D_{AUG} as described in (2), which includes the OCs of the sensors used to acquire D_{FewNew}.

$$D_{\text{AUG}} = \psi(D_{\text{Origin}}) \tag{2}$$

AUG is easier to implement than COR because it does **not** use an OC acquisition device. D_{AUG}, which is obtained by augmenting D_{FewNew} with significantly less data than D_{Origin}, is used in the measurement system composed of target sensors. Moreover, an increase in the ML estimation error can be prevented by using D_{AUG} and not D_{Origin}. As the acquisition time of D_{FewNew} is short, the training data acquisition time can be reduced.

IV. ML-Based Measurement System Used for Evaluation Experiment

A. ML-Based Relative Position and Orientation Measurement Device Using Distance Sensor Array

For evaluation experiments, a relative position and orientation measurement device was used. Fukui et al. developed a relative position and orientation measurement device for platooning small cars [19]. As shown in Fig. 4, the device consists of a hexagonal ring and octagonal pin with eight distance sensors (SHARP, GP2Y0E02B [20]) on each face. The training data are the relative position and orientation (x, y, θ) of the pin in the ring, and distance data $\boldsymbol{L}(L_{(1)} \cdots L_{(8)})$ are measured at that position. The eight distance sensors measure distance $\boldsymbol{L}$ to the wall of the ring. The position and orientation, (x, y, θ), are estimated using the k-nearest neighbor (k-NN) method in the feature space consisting of $\boldsymbol{L}$. k-NN is an ML algorithm that easily reflects the characteristics of the training data because it utilizes the distribution of the training data in the feature space of

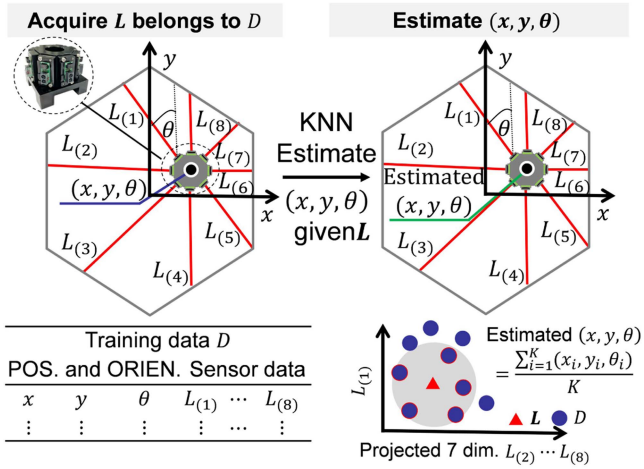

Fig. 4. Relative position and orientation measurement device.

TABLE I
Training Data Acquisition Conditions

	Position		Orientation	Sensor outputs	Time
	x (mm)	y (mm)	θ (deg)	$\boldsymbol{L}$ (-)	2160 mins
Range	-200~200	-230~230	-29~29	L_1~L_8	No. of data
Pitch	5	5	1		3.63×10^6

$\boldsymbol{L}$. Therefore, the analysis of the results when using the training data obtained from the proposed method is straightforward.

The estimated errors from the true position and orientation are evaluated using the root-mean-square error (RMSE) as follows:

$$\text{RMSE} = \sqrt{(1/N)\sum_{i=1}^{N} e_i^2} \tag{3}$$

Here, e_i represents the error between the estimated value obtained using k-NN and true value, and N represents the number of measurement points on the x, y, and θ axes. On the other hand, when drawing the RMSE distribution in a ring, N is the number of measurement points on the θ axis.

B. Experiment to Verify Decrease in Estimation Accuracy During DT

The estimation accuracy is expected to decrease when the training data acquired using the original sensors are directly transferred to a measurement system comprising other sensors. In this experiment, the decrease in the estimation accuracy in DT when using the relative position and orientation measurement device was investigated. The results were used as the criteria for evaluating the results of the evaluation experiments for each proposed method.

1) Experimental Conditions: Training data D_i for the experiment were acquired from sensors S_i, where $i \in A, B, C$. The same sensors and training data were used in the evaluation experiments. The training data acquisition conditions are shown in Table I. The pin was moved under the conditions shown in Table I, and the training data were acquired by associating position and orientation (x, y, θ) of the pin with distance data $\boldsymbol{L}$

IEEE Robotics and Automation Letters (RA-L) paper, presented at ICRA 2026, Vienna, Austria. Cite as RA-L paper.

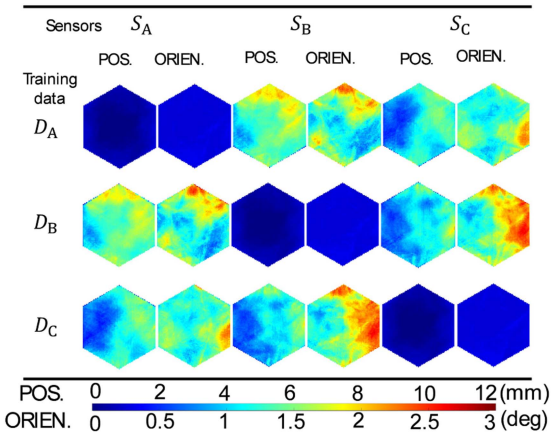

Fig. 5. RMSE distribution of pin relative position and orientation in ring when reusing training data.

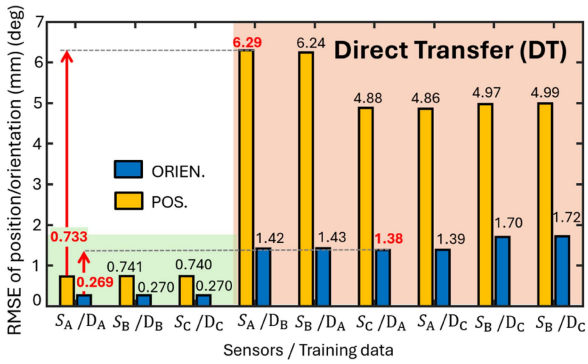

Fig. 6. RMSE of pin relative position and orientation in ring when reusing training data.

. The training data acquisition time for the relative position and orientation measurement devices was approximately 36 h. The acquisition dates of D_{A} and D_{B} were approximately 2 months apart from those of D_{C} for experimental convenience.

2) Experimental Results: Fig. 5 shows the distribution of the estimated RMSE of the pin relative position and orientation in the ring when using training data D_{A}, D_{B}, and D_{C} from sensors S_{A}, S_{B}, and S_{C}, respectively. At each point on the x and y axes in the ring, the RMSE of all the estimated data obtained by changing θ is shown. The pitch of the estimated data acquisition on the x, y, and θ axes is the same as that in Table I. The distribution is shown in blue when the RMSE of the relative position and orientation in the ring is low, indicating high-accuracy estimation, and in red when the accuracy is low.

The RMSE distribution of the pin position and orientation when using each of the training data in the relative position and orientation measurement device with sensors that acquired it (RMSE distributions are placed diagonally in Fig. 5) is blue and small throughout the ring. Conversely, the RMSE distribution of the pin position and orientation, when reusing each of the training data in the relative position and orientation measurement device with sensors that did not acquire the training data, increases drastically throughout the ring. Fig. 6 shows the RMSE of all the estimated data obtained in the ring. The results for the normal training data of $S_{\mathrm{A}}/D_{\mathrm{A}}$, $S_{\mathrm{B}}/D_{\mathrm{B}}$, and $S_{\mathrm{C}}/D_{\mathrm{C}}$ highlighted in green are compared with the results of DT highlighted in red. The RMSE of the position and orientation increase by approximately six to eight times due to the difference in OCs between the training data and the sensor used for the measurement. Although the distances measured by the sensors and object tilt are the same, the distances measured by each sensor can differ. Consequently, the relationship between the distance, position, and orientation associated with the training data depends on the OC of the sensor used, which considerably increases the RMSE. In addition, because the relative position and orientation measurement device uses k-NN, the distribution of distance data $\boldsymbol{L}$ obtained from the sensor and that of the neighboring training data in the feature space significantly impacts the estimation accuracy. For DT, the distribution of the neighboring training data of distance data $\boldsymbol{L}$ obtained from the sensor changes, and the estimation accuracy decreases.

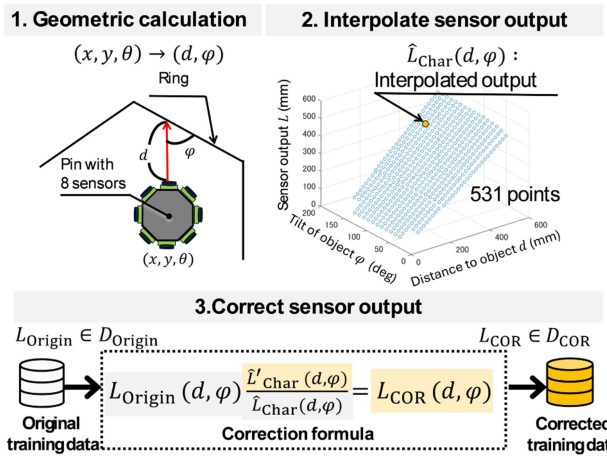

Fig. 7. Implementation of training data correction (COR) approach.

In the following sections, the average position and orientation RMSE of 5.37 and 1.51, respectively, which are the results of the six trials of DT, are used baseline for performance evaluation of the proposed method.

V. Implementation of Training Data Correction and Evaluation Experiment

A. Implementation of Training Data Correction

Fig. 7 shows the implementation of COR. This approach corrects the OCs included in the original training data, D_{Origin}, to obtain D_{COR}.

As shown in the upper-left graph of Fig. 7, distance d and tilt φ of the ring wall measured by each sensor are geometrically calculated from (x, y, θ) associated with distance data L_{Origin} in D_{Origin}. This calculation shows conditions under which L_{Origin} in D_{Origin} is obtained, that is, distance d to the object and tilt φ of the object. To correct the value of $L_{\mathrm{Origin}}(d, \varphi)$, the OC data of the target and original acquisition sensors are required. The OC acquisition device gathers the OC data of eight sensors for approximately 30 min by changing the distance and tilt of the object by actuators. As the OC data obtained by this device are discrete, OC data $\hat{L}_{\mathrm{Char}}(d, \varphi)$ for arbitrary d, φ is calculated

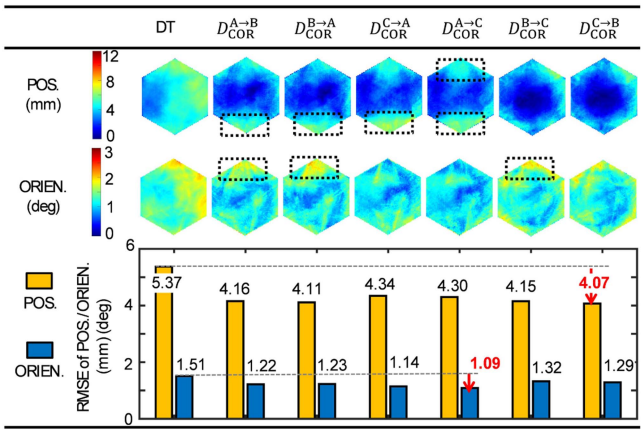

Fig. 8. RMSE distribution of pin relative position and orientation in ring with training data correction.

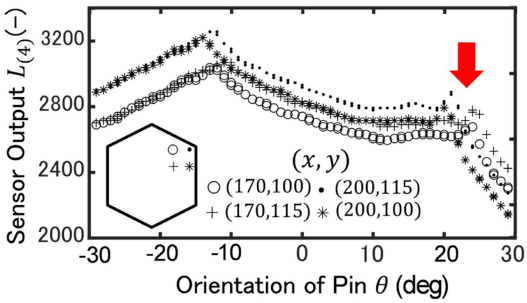

Fig. 9. Transition of distance data when pin orientation is changed at ring corner.

using the natural neighbor interpolation. The OC data obtained using the OC acquisition device are derived by including the convex hull of d, φ geometrically calculated from the training data, thus enabling interpolation. OC data $\hat{L}'_{\mathrm{Char}}(d,\varphi)$ of the target sensors and $\hat{L}_{\mathrm{Char}}(d,\varphi)$ of the original sensors obtained by interpolation are used to correct $L_{\mathrm{Origin}}(d,\varphi)$ using (1).

This correction is applied to each L_{Origin} value in D_{Origin} to obtain D_{COR}.

B. Evaluation Experiment of Training Data Correction

The OC of S_i were included in D_i that aimed at the OCs of S_j through correction. To test all two-item combinations of A, B, and C, six iterations of training data conversion were executed per experimental condition. Training data $D_{\mathrm{COR}}^{i\to j}$ obtained after correction were used in the relative position and orientation measurement device composed of S_j.

Fig. 8 shows the RMSE distribution of the pin relative position and orientation inside the ring in the training data correction experiment. Compared to DT, the corrected training data makes the blue stand out in the RMSE distribution of the pin position and orientation in the ring. In addition, the pin position and orientation RMSE decreases in all trials compared with DT by up to 23% and 28%, respectively.

However, at the dashed box in Fig. 8, the RMSE distribution increases despite correction. This is due to other reflections near the measurement target in the area indicated by the dashed box in the ring. Fig. 9 shows the change in the distance data $L_{(4)}$ when changing the pin orientation at four points near the vertex of the ring in the training data. The vertical axis represents distance $L_{(4)}$ in the training data, and the horizontal axis represents pin orientation θ. The arrow in Fig. 9 indicates that the data are scattered widely near the vertex of the ring; thus, data continuity is impaired. Distance sensors on this device are subjected to multiple reflections of the emitted light of sensors near the vertex of the ring, which affects the sensor data, making the OCs more complex.

The RMSE reduction rate when using the corrected training data with respect to the RMSE of DT is low for all trials. This is because the OC data of all the sensors, comprising a distance sensor array, are acquired at the same distance, d, and tilt, φ. This indicates that the correction is less dependent on the difference in OCs between the training data, even under large differences in OCs across training data.

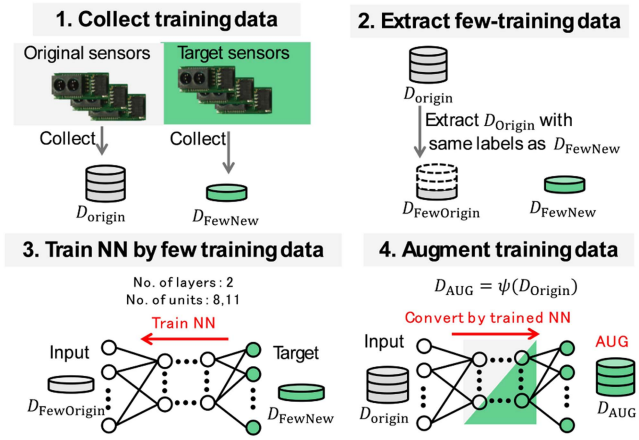

Fig. 10. Implementation of few-training data augmentation approach.

VI. Implementation of Few-Training Data Augmentation and Evaluation Experiment

A. Implementation of Few-Training Data Augmentation

Fig. 10 shows the AUG implementation. First, training data D_{FewNew} were acquired using the target sensors for approximately 10 min. Then, $D_{\mathrm{FewOrigin}}$ was obtained by extracting data from training data D_{Origin} that exactly matched (x, y, θ) in D_{FewNew}.

An NN approximated multi-input and multi-output mapping function ψ between the two training sets in a data-driven manner, with $D_{\mathrm{FewOrigin}}$ and D_{FewNew} being the input and output data, respectively. The NN had two hidden layers of eight and eleven units. NN training for this evaluation experiment converged within tens of seconds in all cases.

When D_{Origin} is entered into approximated mapping function ψ obtained by the NN, as shown in (2), the output is D_{AUG} and contains the OC of the target sensors.

B. Evaluation Experiment of Few-Training Data Augmentation

This section describes the experiment on the mutual conversion of training data to evaluate the AUG approach. NN training

IEEE Robotics and Automation Letters (RA-L) paper, presented at ICRA 2026, Vienna, Austria. Cite as RA-L paper.

TABLE II
VARIATIONS OF FEW-TRAINING DATA

	Extremely sparse	Sparse	Reference	Dense	Center-biased	Extremely dense	d-φ random (Sparse)	d-φ random (Reference)	d-φ random (Dense)
No. of training data for NN	297	495	693	2574	2673	4488	616	2519	4312
Collection time (mins)	4	6	8.4	31	32	54	8	31	52
Data pitch									

was intended to obtain function ψ to satisfy (4).

$$D_{\text{FewNew}} \approx \psi(D_{\text{FewOrigin}})$$
$$D_{\text{FewOrigin}} \in D_i, D_{\text{FewNew}} \in D_j \tag{4}$$
$$D_{\text{AUG}}^{i\to j} = \psi(D_i) \tag{5}$$

Then, (2) could be written as in (5). $D_{\text{AUG}}^{i\to j}$ containing the OC of S_j was obtained from D_i. The generated $D_{\text{AUG}}^{i\to j}$ was used in the relative position and orientation measurement device composed of S_j, and the estimation results of the positions and orientations of the pins were evaluated in terms of RMSE.

AUG approximates the mapping function using a set of training data acquired in a short time from the target sensors and a portion of the training data collected from the original sensors. It is important to approximate the mapping function with high accuracy using a small batch of training data. Therefore, the conversion accuracy is compared with various training data by approximating the mapping function to provide guidelines for acquiring fewer training data.

1) Experimental Conditions: In this experiment, the mapping function was approximated using different few-training datasets in an NN. The converted training data were evaluated for conversion accuracy based on the position and orientation RMSE in the ring using the approximated mapping function. The original and target training data were D_i and D_j, respectively. The training data converted for the augmentation of the few-training data were $D_{\text{AUG}}^{i\to j}$. The training data used for this experiment were the same as those in the previous experiments. The few-training data for approximating the mapping function are explained in Table II. The few-training data were prepared for extremely sparse, sparse, and reference data, which could be acquired in less than 10 min. In addition, three methods for acquiring few-training data that could be acquired in approximately 30 min, namely, dense and center-biased, were prepared. The extremely dense datasets could be collected in approximately 5 0 min and were uniformly and more densely acquired in the ring compared with the dense datasets.

It is important to use distance data $\boldsymbol{L}$ obtained at various distances d and tilts φ of the object to accurately approximate the distance sensor OCs using the NN. Fig. 11 shows distance d and tilt φ geometrically calculated from the distance data L obtained in the few-training data of reference and d–φ random. Compared with the reference, d–φ random can acquire distance data over a wide range on the d–φ plane. Three sets of few-training data

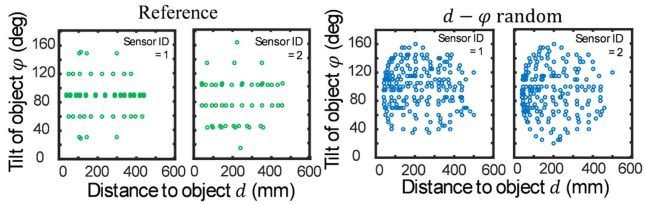

Fig. 11. d–φ plane of OC data.

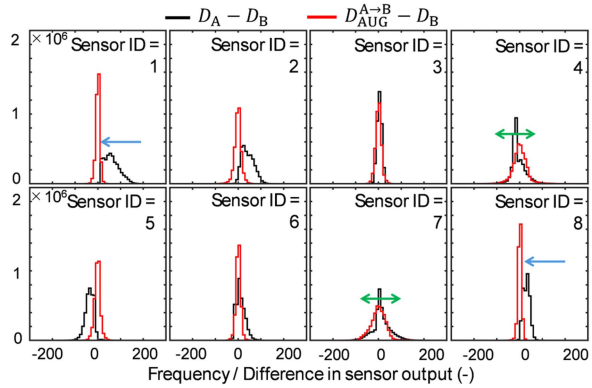

Fig. 12. Error distribution between original and augmented training data.

from the right shown in Table II were prepared by using the d–φ random method to compare with datasets that had almost the same amount of data.

2) Experimental Results: First, we show how AUG conversion changes the output values of the sensors. Fig. 12 shows the error distribution of the training data before and after conversion using the mapping function constructed using the reference datasets. Fig. 12 shows the error distribution with D_{A} before conversion, D_{B} acquired by the target sensors S_{B}, and training data $D_{\text{AUG}}^{\text{A}\to\text{B}}$ converted using mapping function ψ as the true value. By comparing the error distribution between D_{Target} (D_{B}) and D_{Origin} (D_{A}) with that between D_{Target} and $D_{\text{AUG}}^{\text{A}\to\text{B}}$, the peak of the error distribution of $D_{\text{AUG}}^{\text{A}\to\text{B}}$ is closer to 0in the sensor with ID 1 or 8. Alternatively, the tail of the distribution is widened by the conversion in the sensor with ID 4 or 7. In the sensor with ID 1 or 8, the kurtosis of the error distribution is high. In contrast, in the sensor with ID 4 or 7, the standard deviation of the error after conversion increases. This reveals that a single multi-input and multi-output mapping function constructed using the few-training data alone cannot convert

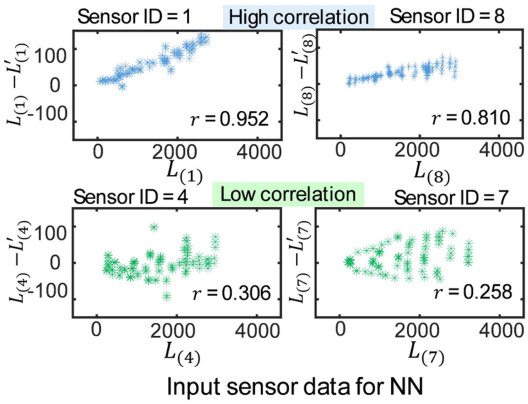

Fig. 13. Correlation between original and augmented training data used in NN.

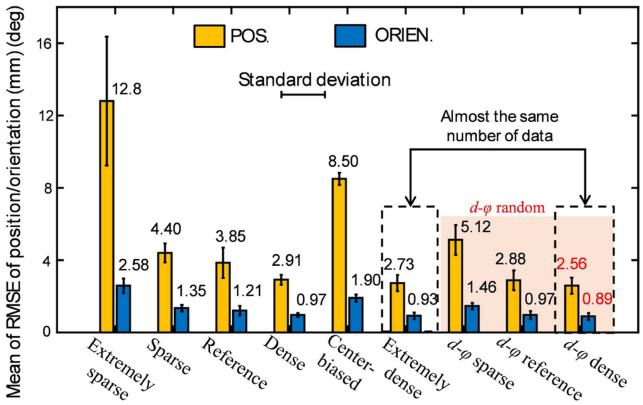

Fig. 14. Comparison of RMSE distribution of pin relative position and orientation in ring for different few-training data.

all the sensor values in the training data with the same level of accuracy.

Fig. 13 shows the scatter plot between the different few-training data used in NN learning. The horizontal axis represents sensor data L in a small batch of D_{A}. The vertical axis represents the difference between L in a small batch of D_{A} and L' in a small batch of D_{B}. In Fig. 12, the sensor with ID 1 or 8 shows a high kurtosis of the error distribution owing to the conversion, and correlation coefficient r is higher than 0.8. In contrast, the sensor with ID 4 or 7 shows a low correlation coefficient r of approximately 0.3. Consequently, the NN struggles to accurately approximate the mapping function between sensors with complex relationships, such as the sensors with IDs 4 and 7. Moreover, the approximation accuracy of the mapping function does not improve despite the amount of data increasing for conversion between sensors with complex relationships because the NN has a low expressive capability. Therefore, the difference in the OCs of the sensor affects the ease of approximating the mapping function.

We discuss the accuracy of the NN conversions for the different sets of few-training data. Fig. 14 compares the mean RMSE in the ring when the mapping function is approximated using various few-training data shown in Table II. The mean and standard deviation were calculated based on the RMSE of

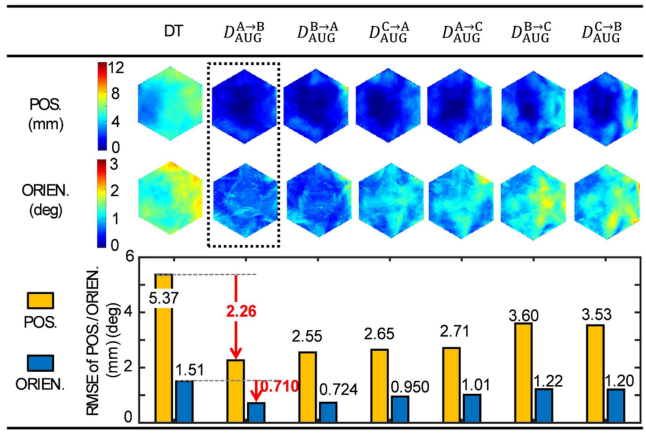

Fig. 15. RMSE distribution of pin relative position and orientation in ring when few-training data are augmented.

six training data conversions using three training sets (D_{A}, D_{B}, and D_{C}). The few-training data for NN can be acquired in two ways, one determined based on the coordinates in the ring and the other based on the coordinates on the d–φ plane. Except for center-biased, which collects extremely biased data in the plane, the RMSE tends to decrease as the amount of data increases for both methods. However, for the extremely dense and d–φ dense, which have the same amount of few-training data, the mean of d-φ dense is smaller. This is because the distribution of data on the d–φ plane is biased, even though the distribution of the few-training data in the ring is increased. Therefore, the structures of the few-training data that simply increase the data in the ring prevent the approximation of the mapping functions with high conversion accuracy. In other words, constructing a small quantity of training data in a way that gives the NN various data of OCs leads to more accurate conversions.

Fig. 15 shows the RMSE distribution of the pin position and orientation when the training data is converted to include the OC of the used sensor. We used training data $D_{\mathrm{AUG}}^{i\to j}$ converted by the mapping function ψ approximated by d-φ reference. Few-training data, d–φ reference, could be obtained in about 30 min, which was almost the same time as that for the collection of the OC data for the COR method. Compared with the position and orientation RMSE of DT, the RMSE distribution of the pin position and orientation in the ring is noticeable in blue in all trials, and the error is reduced. Additionally, in the trials of $D_{\mathrm{AUG}}^{\mathrm{A}\to\mathrm{B}}$, blue is noticeable throughout the ring, and the position and orientation RMSE are drastically reduced. The bar graph at the bottom of Fig. 15 demonstrates that the RMSE of the pin position and orientation decreases in all conversions compared with the pin position and orientation RMSE of DT. This implies that the training data converted to include the OCs of different sensors are created using mapping function ψ approximated using the few-training data. The position and orientation RMSE values are reduced by approximately 58% and 53%, respectively, compared with those of DT. In contrast, there is a variation in the RMSE reduction rate of each trial against the position and orientation RMSE values of DT. This is because, as mentioned above, the difference in the sensor OCs affects the

IEEE Robotics and Automation Letters (RA-L) paper, presented at ICRA 2026, Vienna, Austria. Cite as RA-L paper.

ease of approximating the mapping function. In future work, a method for constructing a mapping function that can accurately convert the difference in OCs between each sensor, even when the difference is complex, will be developed.

VII. Conclusion

Distance sensor arrays have been proposed for various applications because they are inexpensive, and ML can be leveraged to estimate quantities that are impossible to measure directly using sensor arrays alone. In this study, two methods were proposed for alleviating the training data acquisition process by converting sensor OCs. An experiment was conducted using a relative position and orientation measurement device with an infrared distance sensor array. The approach to correct the training data based on OC data of original acquisition and target sensors achieved a maximum reduction of 23% compared with the position RMSE of DT. The approach to convert the training data using mapping functions reduced the position RMSE by a maximum of 58% compared with DT. It was revealed that it is important to construct few-training data using distance data obtained at various distances and tilts of the object to approximate the mapping function with high accuracy. This study may contribute to the realization of simple and fast calibration methods and the feasibility of employing ML with distance sensor arrays. The results presented in this letter demonstrate the possibility that training data conversion can be used with other optical sensors by considering the important OCs of sensors, such as distance and tilt. Nevertheless, the influence of different measurement surfaces should be verified for other applications. In addition to the sensors that were used in this study, the proposed methods may be applied to other sensors with similar measurement principles, such as ultrasonic distance sensors.

References

[1] S. E. Navarro et al., "Proximity perception in human-centered robotics: A survey on sensing systems and applications," *IEEE Trans. Robot.*, vol. 38, no. 3, pp. 1599–1620, Jun. 2022.

[2] C. Abah, A. L. Orekhov, G. L. h. Johnston, P. Yin, H. Choset, and N. Simaan, "A multi-modal sensor array for safe human-robot interaction and mapping," in *Proc. Int. Conf. Robot. Automat.*, 2019, pp. 3768–3774.

[3] N. M. Ceriani, G. Buizza Avanzini, A. M. Zanchettin, L. Bascetta, and P. Rocco, "Optimal placement of spots in distributed proximity sensors for safe human-robot interaction," in *Proc. IEEE Int. Conf. Robot. Automat.*, 2013, pp. 5858–5863.

[4] G. Buizza Avanzini, N. M. Ceriani, A. M. Zanchettin, P. Rocco, and L. Bascetta, "Safety control of industrial robots based on a distributed distance sensor," *IEEE Trans. Control Syst. Technol.*, vol. 22, no. 6, pp. 2127–2140, Nov. 2014.

[5] S. Hosono, S. Nishimura, K. Iwasaki, and E. Tamaki, "A method for estimating the load on muscles using a wearable IR sensor array device," in *Proc. 2nd Int. Conf. Sensors, Signal Image Process.*, 2019, pp. 77–81.

[6] R. Fukui, H. Ifuku, M. Watanabe, M. Shimosaka, and T. Sato, "Easy-to-install system for daily walking ability assessment using a distance sensor array," *J. Ambient Intell. Smart Environments*, vol. 7, pp. 375–387, 2015.

[7] X. Jiang, Y. Chen, J. Liu, G. R. Hayes, L. Hu, and J. Shen, "AIR: Recognizing activity through IR-based distance sensing on feet," in *Proc. ACM Int. Joint Conf. Pervasive Ubiquitous Comput., Adjunct*, 2016, pp. 97–100.

[8] T. Mitani, S. Okishiba, N. Tateyama, K. Yamanojo, S. Warisawa, and R. Fukui, "A wearable multi-joint wrist contour measuring device for hand shape recognition," *IEEE Robot. Automat. Lett.*, vol. 7, no. 3, pp. 8331–8338, Jul. 2022.

[9] K. Kato, K. Matsumura, and Y. Sugiura, "Aroundsense: An input method for gestures around a smartphone," in *Proc. 26th Int. Display Workshops*, 2019, pp. 1700–1703.

[10] K. Yamashita, T. Kikuchi, K. Masai, B. H. Thomas, M. Sugimoto, and Y. Sugiura, "Cheekinput: Turning your cheek into an input surface by embedded optical sensors on a head-mounted display," *Trans. Hum. Interface Soc.*, vol. 20, no. 3, pp. 311–320, 2018.

[11] S. Amagai, Q. Ye, Y. Fukuoka, S. Warisawa, and R. Fukui, "Clustering of distance sensors to transfer training data for relative position and orientation measurement devices," *ROBOMECH J.*, vol. 9, no. 1, Sep. 2022, Art. no. 20.

[12] Y. Wang, Q. Yao, J. T. Kwok, and L. M. Ni, "Generalizing from a few examples: A survey on few-shot learning," *ACM Comput. Surv.*, vol. 53, no. 3, pp. 1–34, 2020.

[13] F. Zhuang et al., "A comprehensive survey on transfer learning," *Proc. IEEE*, vol. 109, no. 1, pp. 43–76, Jan. 2021.

[14] D. Xu, Z. Zhang, and J. Shi, "A new multi-sensor stream data augmentation method for imbalanced learning in complex manufacturing process," *Sensors*, vol. 22, no. 11, 2022, Art. no. 4042.

[15] J. Yun, D. Kim, D. M. Kim, T. Song, and J. Woo, "GAN-based sensor data augmentation: Application for counting moving people and detecting directions using PIR sensors," *Eng. Appl. Artif. Intell.*, vol. 117, 2023, Art. no. 105508.

[16] J. Wang, T. Zhu, J. Gan, L. L. Chen, H. Ning, and Y. Wan, "Sensor data augmentation by resampling in contrastive learning for human activity recognition," *IEEE Sensors J.*, vol. 22, no. 23, pp. 22994–23008, Dec. 2022.

[17] Y. Shi, X. Ying, and J. Yang, "Deep unsupervised domain adaptation with time series sensor data: A survey," *Sensors*, vol. 22, no. 15, 2022, Art. no. 5507.

[18] F. Li, K. Shirahama, M. A. Nisar, X. Huang, and M. Grzegorzek, "Deep transfer learning for time series data based on sensor modality classification," *Sensors*, vol. 20, no. 15, 2020, Art. no. 4271.

[19] R. Fukui and Y. Okamoto, "Hils-based development of a relative position and orientation measurement system for platooning vehicles with coupling devices," *SICE J. Control, Meas., Syst. Integration*, vol. 11, no. 4, pp. 274–283, 2018.

[20] Sharp, "GP2Y0E02 A, GP2Y0E02B, GP2Y0E03 application note," May 14, 2025. [Online]. Available: https://global.sharp/products/device/lineup/data/pdf/datasheet/gp2y0e02_03_appl_e.pdf